Received: 31 October 2018 | Revised: 28 June 2019 | Accepted: 19 July 2019

DOI: 10.1002/term.2948

RESEARCH ARTICLE

WILEY

Load-induced osteogenic differentiation of mesenchymal stromal cells is caused by mechano-regulated autocrine signaling

Sophie Schreivogel[1,2] | Virinchi Kuchibhotla[1] | Petra Knaus[2,4] | Georg N. Duda[1,2,3] | Ansgar Petersen[1,2,3]

[1] Julius Wolff Institute, Charité – Universitätsmedizin Berlin, Berlin, Germany

[2] Berlin-Brandenburg Center and School for Regenerative Therapies, Berlin, Germany

[3] Center for Musculoskeletal Surgery, Charité - Universitätsmedizin Berlin, Berlin, Germany

[4] Institute for Chemistry and Biochemistry, Freie Universität Berlin, Berlin, Germany

Correspondence
Dr. rer. nat. Ansgar Petersen, Charité – Universitätsmedizin Berlin, Julius Wolff Institut, Augustenburger Platz 1, D-13353 Berlin
Email: ansgar.petersen@charite.de

Funding information
German Research Foundation, Grant/Award Number: # PE 1802/1-1; RMS Foundation, Grant/Award Number: E11_0009: 3D scaff-stiff

Abstract

Mechanical boundary conditions critically influence the bone healing process. In this context, previous *in vitro* studies have demonstrated that cyclic mechanical compression alters migration and triggers osteogenesis of mesenchymal stromal cells (MSC), both processes being relevant to healing. However, it remains unclear whether this mechanosensitivity is a direct consequence of cyclic compression, an indirect effect of altered supply or a specific modulation of autocrine bone morphogenetic protein (BMP) signaling. Here, we investigate the influence of cyclic mechanical compression (ε = 5% and 10%, f = 1 Hz) on human bone marrow MSC (hBMSC) migration and osteogenic differentiation in a 3D biomaterial scaffold, an *in vitro* system mimicking the mechanical environment of the early bone healing phase. The open-porous architecture of the scaffold ensured sufficient supply even without cyclic compression, minimizing load-associated supply alterations. Furthermore, a large culture medium volume in relation to the cell number diminished autocrine signaling. Migration of hBMSCs was significantly downregulated under cyclic compression. Surprisingly, a decrease in migration was not associated with increased osteogenic differentiation of hBMSCs, as the expression of RUNX2 and osteocalcin decreased. In contrast, BMP2 expression was significantly upregulated. Enabling autocrine stimulation by increasing the cell-to-medium ratio in the bioreactor finally resulted in a significant upregulation of RUNX2 in response to cyclic compression, which could be reversed by rhNoggin treatment. The results indicate that osteogenesis is promoted by cyclic compression when cells condition their environment with BMP. Our findings highlight the importance of mutual interactions between mechanical forces and BMP signaling in controlling osteogenic differentiation.

KEYWORDS

autocrine signaling, bioreactor, bone morphogenetic protein type 2, cell migration, mechanical loading, osteogenic differentiation

1 | INTRODUCTION

Bone fracture healing is a complex multistage process that depends on coordinated biochemical and biomechanical signals. The relevance of mechanical boundary conditions for fast and successful bone regeneration has been documented earlier (Betts & Müller, 2014; Duda et al., 2001). Due to the gained knowledge, fracture fixation systems nowadays aim to account for proper mechanobiological requirements (Märdian, Schaser, Duda, & Heyland, 2015). Interfragmentary movements at the fracture site are differentiated in axial compression of fracture fragments or relative movements resulting in shear. Whereas shear stress is widely considered detrimental, it is commonly accepted that a distinct amount of compression promotes bone regeneration and too little or too large axial movements delay healing (Claes & Heigele, 1999; Epari, Taylor, Heller, & Duda, 2006; Mehta, Duda, Perka, & Strube, 2011). Specifically, the early phase of the healing cascade is considered to be highly mechanosensitive (Klein et al., 2003). In this regard, we and others suggested that the initial mechanical condition influence the entire subsequent inflammatory, angiogenic, and endochondral healing cascades (Goodship, Cunningham, & Kenwright, 1998; Klein et al., 2003; Schell et al., 2005). To further employ the power of mechanobiology in critical healing scenarios, an improved understanding of how mechanical stimuli influence cellular processes like migration, differentiation, and growth factor signaling is needed.

Following this motivation, various test systems for the *in vitro* application of mechanical stimulation have been developed, including force application in cell culture well plates (Michalopoulos et al., 2012; Shin Kang et al., 2013; Sittichokechaiwut, Edwards, Scutt, & Reilly, 2010) or bioreactors (Jagodzinski et al., 2008; Kopf, Petersen, Duda, & Knaus, 2012; Ode et al., 2011; Petersen, Joly, Bergmann, Korus, & Duda, 2012). Diverse effects of mechanical stimulation on cell migration were reported. Although osteoblasts on cyclically strained 2D membranes showed an enhanced migration capacity (Bhatt et al., 2007), migration of MSCs embedded in a hydrogel was reduced in response to cyclic compression (Ode et al., 2011). Progenitor cells migrate from intact bone regions with low strain into the fracture side with high strain (Gerstenfeld, Cullinane, Barnes, Graves, & Einhorn, 2003; Klosterhoff et al., 2017) where their differentiation is controlled by the mechanobiological environment. Thus, it is of relevance to investigate potential alterations in progenitor cell migration and differentiation in response to different strain regimes. Multiple studies examined the influence of loading on stem cell differentiation, particularly osteogenic commitment (reviewed in Delaine-Smith & Reilly, 2011). Motivated by a tissue engineering approach, the majority of these studies used osteoinductive medium supplements or bone-derived scaffolds masking effects of loading on cell fate decision.

However, studies that worked without additional osteogenic triggers reported on an induction of osteogenic differentiation by cyclic bulk material deformation (f = 1 Hz), reflected by an increased expression of Runt-related transcription factor 2 (RUNX2; Michalopoulos et al., 2012), Alkaline phosphatase (ALP), and osteopontin (Shin Kang et al., 2013) in human MSCs. Interestingly, mechanical loading was previously shown to induce the expression of bone morphogenetic protein type 2 (BMP2) in MSCs (Wang et al., 2010). The growth factor is a potent inducer of bone formation and indispensable for fracture healing (Tsuji et al., 2006). The instance that it induces the expression of RUNX2 (Lee et al., 2000) points toward an involvement of BMP-signaling in load-induced osteogenic differentiation. However, if the observed pro-osteogenic effects of cyclic compression on MSCs are a consequence of mechanoregulated gene expression or an indirect consequence of load-induced autocrine or paracrine signaling (e.g., via secretion and signaling of BMP2) remains an open question.

With the present study, we aimed at investigating the direct influence of cyclic mechanical loading on the migration and osteogenic differentiation of primary hBMSCs. Based on the predominant opinion in the literature available for MSCs, we hypothesized that cyclic mechanical loading can directly induce osteogenic differentiation and consequently influence cell migration. However, the fact that key osteogenic genes and especially RUNX2 were downregulated in response to cyclic compression, but BMP2, on the other hand, was clearly upregulated, advised us to consider the indirect load-induced autocrine BMP signaling as a mediator of osteogenic gene expression under cyclic compression.

2 | MATERIALS AND METHODS

2.1 | Collagen scaffolds used as cell carriers

Macroporous scaffolds from porcine collagen were utilized as a 3D cell carrier material in this study (in cooperation with Matricel GmbH, Herzogenrath, Germany). Two scaffold prototypes with collagen contents of 1.1 and 1.5 wt-% were produced via directional freezing and freeze drying leading to elastic moduli of 3.4(±0.9) kPa (scaffold A) and 12.3(±1.8) kPa (scaffold B), respectively. The scaffolds were characterized by highly aligned channel-like pores with vertical pore orientation, providing nutrient and oxygen supply and at the same time offering a guiding structure for cell migration. As shown before, the differences in collagen content did not affect the pore size (1.1 wt-% = 76 μm ± 12 μm, 1.5 wt-% = 79 μm ±14 μm) and architecture as analyzed using electron microscopy (Herrera et al., 2019; Petersen et al., 2012). In brief, three rectangular scaffolds have been cut from different regions of the bulk material with the collagen content of 1.1 or 1.5 wt-%. Electron microscopy images at three different positions have been taken from the scaffolds in top view. Scaffold pore diameter was measured using a custom-made ImageJ plugin calculating the average distance between two scaffold pores. Therefore, two scaffold walls confining a scaffold pore were contoured manually in one image, and the mean pore diameter was calculated for at least three pores per image. For cell culture experiments, cylindrical shaped scaffolds with a diameter of 5 mm and a height of 3 mm were prepared.

2.2 | Bioreactor and mechanical loading parameters to mimic the early bone healing phase

A custom-made mechanobioreactor system, previously described by Petersen et al. (2012) was used to apply cyclic monoaxial compression to the cell-seeded scaffolds with pores oriented in the axial direction (Figures 1b and 1c). The system was designed to mimic the mechanical environment in the hematoma during the early phase of fracture healing. In brief, the bioreactor can be separated in two compartments, the cell culture unit and the mechanical unit. The cell culture unit can be assembled under sterile conditions and consists of a reactor chamber, a medium reservoir allowing gas exchange and a micro pump (pump rate approx. 2.5 ml/min). The micro pump is circulating the medium and is necessary for a sufficient supply of the cells inside the 3D biomaterial. The pump is running in all experimental conditions, also under control conditions (no cyclic compression). In comparison with static culture in well plates, the system provides an enhanced fluid flow in the reactor chamber. The mechanical unit allows the application of defined loading patterns and the online measurement of the force acting on the sample. The scaffold inside the reactor chamber was subjected to a sine wave of cyclic monoaxial compression with a frequency of 1 Hz and a magnitude of 5 or 10% scaffold height (150 and 300 μm, respectively). Cyclic mechanical compression was applied periodically with 3-hr stimulation and 5-hr break in the direction of the scaffold pores. The loading parameters were selected to represent the *in vivo* loading situation (see Section 4).

2.3 | Cells and culture medium

Primary human mesenchymal stromal cells (hBMSCs) isolated from bone marrow of eight patients who underwent total hip endoprothesis were used in passages 3 to 5. Cells were expanded in Dulbecco's modified Eagle's medium (DMEM, D5546, Sigma Aldrich, St. Louis, USA) supplemented with 10 vol-% fetal bovine serum (# S 0115; Biochrom AG, Berlin, Germany), 1 vol-% penicillin/streptomycin (# A 2213; Biochrom AG, Berlin, Germany), and 1 vol-% Glutamax (35050–038, Life Technologies, Carlsbad, USA) under 5% CO_2 in a humid incubator. The osteogenic differentiation potential was verified for each patient measuring the ALP activity and calcium phosphate precipitation using differentiation medium supplemented with 50 μM L-ascorbic acid 2-phosphate (AA, K0293, Biochrom AG, Berlin, Germany), 10 mM β-Glycerolphosphate (11011375001, Roche, Basel, Switzerland), and 100 nM Dexamethasone (D2915-100G, Sigma Aldrich).

2.4 | Homogeneous cell seeding in collagen scaffolds

After expansion, cells were trypsinized and a cell concentration of 2.5×10^3 cells/μl was adjusted, which corresponds to a cell density of approximately 1.5×10^5 cells/scaffold. Collagen scaffolds were dipped into the cell suspension where the scaffold immediately soaked up suspension until completely filled and were subsequently transferred into a 12-well culture plate. During an incubation of 60 min at 37°C, cells were allowed to adhere to the scaffold walls. Subsequently, cell-seeded constructs were washed once in cell culture medium to remove unattached cells and placed into a new 12-well plate filled with 1.4 ml cell culture medium. After 24 hr of incubation, the scaffolds were transferred into the bioreactor. As shown previously, uniform distribution of cells within the scaffold was achieved using this seeding method (Brauer et al., 2019).

2.5 | Fluorescent staining and imaging

Cells were fixed in 4% paraformaldehyde and quenched for 1 hr in a 50-mM ammonium chloride solution. Thereafter, the scaffolds were infiltrated with 5% gelatin solution at 37°C, which was subsequently solidified at 4°C to stabilize the scaffold structure; gentle cutting along the symmetry axis was enabled. Prior to fluorescence staining, gelatin was washed out by incubation in phosphate-buffered saline (PBS) at 37°C. Right before the staining, three washing steps with TBS-T (40 mM Tris hydrochloride, 10 mM Trizma® base, 150 mM sodium chloride, 0.025% Triton-X 100, pH 8.2) were conducted. The F-actin cytoskeleton was stained with Phalloidin-Alexa 488 (# A12379, Life Technologies, Carlsbad, CA, USA) and cell nuclei were stained with 4′-6-diamidino-2-phenylindiole (DAPI, # D1306, Life Technologies, Carlsbad, CA, USA). Images were taken using a Leica TCS SP5II confocal multiphoton microscope at 25× magnification.

2.6 | Oxygen concentration measurement inside cell seeded collagen scaffolds

The measurement was performed on the 3rd and 7th day after cell seeding inside the bioreactor. The measurement range of the fiber oxygen microsensor (Implantable Oxygen Microsensor IMP-PSt1, Presens, Germany) was validated in cell culture medium under culture conditions [20.8(+/−0.1)% O_2] and under nitrogen gas [0.2(+/−0.03)% O_2]. The probe was inserted into the upper piston of the bioreactor and the penetration depth of the probe into the scaffold was adjusted computer controlled using the bioreactors piezo drive (Figure S2 in the Supporting Information). Oxygen measurement was performed every 50 μm until the middle of the scaffold (1500 μm).

2.7 | 3D migration assay and analysis of migration distance

The assay was performed as described previously (A. Petersen et al., 2018). In brief, a defined area for cell attachment was created using custom-made silicone rings with an inner diameter of 7 mm and a height of 3 mm, which were placed centrally into a 12-well plate. Cells were brought into suspension in a concentration of 2×10^3 cells/μl, and 104 μl of the suspension was added inside the rings. The cells were allowed to adhere in a multicell layer for 1 hr at 37°C. Thereafter, the silicone rings were removed, and the cell layer was carefully washed twice with PBS. Collagen scaffolds

were dipped into DMEM and placed centrally on the cell multilayer. Subsequently, culture medium was added and the samples were incubated for 24 hr to enable cell migration into the scaffold. On the next day, scaffolds were transferred into the bioreactor or in another 12-well plate and cultured for additional 3 days in migration medium (DMEM, D5546, Sigma Aldrich), 1 vol-% penicillin/streptomycin, 1 vol-% nonessential amino acids (K0293, Biochrom AG, Berlin, Germany), and 1 vol% Nutridoma (14244100, Roche, Basel, Switzerland). The scaffolds were fixed in 4% paraformaldehyde, incubated in ammonium chloride solution (50 mM) and infiltrated by gelatin solution (5%). After solidification of the gelatin the scaffolds were cut along the symmetry axis. The scaffold halves were transferred into a cryomold, embedded in cryoblock (41–3020-00, Medite GmbH, Burgdorf, Germany), and frozen on a liquid nitrogen-cold aluminum bridge. Cryosections of 20-µm thickness were cut using a cryostat (Leica CM3050S) and immobilized on glass slides. Cell nuclei were stained with DAPI and overview images of the sections were taken (Leica DMBR, Leica). A region of interest was defined in the center of the scaffold (width = 3,000 px) and the x/y coordinates of each cell nuclei were obtained using ImageJ. The migration distance was calculated as the difference between Y_0 (edge of the scaffold) and the Y position of the nuclei.

Using this assay, first, the migration ability of hBMSCs under the influence of 5% and 10% cyclic mechanical compression and dependent on the substrate stiffness was investigated. Second, the influence of osteogenic differentiation on the migration capacity of hBMSCs was assessed in the cell culture incubator under static conditions. For this, hBMSCs (five donors) were osteogenically pre-differentiated by treatment with osteogenic medium (OM) in cell culture flasks over 7 days. Subsequently, scaffolds were seeded with these pre-differentiated cells for the 3D migration assay. During the migration experiment (3 days), undifferentiated and pre-differentiated hBMSCs were both cultured in migration medium to exclude a direct influence of osteogenic supplements on cell motility.

2.8 | RNA isolation, reverse transcription, and quantitative real-time PCR

After 6 days of bioreactor culture with and without cyclic compression, cell-seeded scaffolds were snap-frozen on dry ice. Thereafter, scaffolds were mechanically pulverized in the gas phase of liquid nitrogen utilizing a custom-made piston/cylinder device to enhance the RNA yield. Total RNA was isolated and purified using the PureLink® RNA Mini Kit (12183018A, Life Technologies, Carlsbad, USA), and total DNA digestion was performed using On-column PureLink® DNase (12185–010, Invitrogen, Carlsbad, USA). For each sample, 500 ng mRNA were transcribed into cDNA using iScript™ cDNA Synthesis Kit (#170–8891, BIO-RAD, Hercules, USA). Gene expression was measured by SYBR green-based quantitative real-time PCR (qPCR) and calculated using the efficiency corrected $\Delta\Delta C_T$–method. The mean normalized expression ratios were determined using hypoxanthine-guanine phosphoribosyl transferase 1 (*HPRT1*) as the reference housekeeping gene. The sequences of all primer are deposited in Table 1. Gene expression of cells treated with 5% or 10% cyclic compression and seeded in 3.4 kPa or 12.3 kPa scaffolds were normalized to the noncompressed control of the respective scaffold type.

2.9 | Quantitative measurement of hBMP2 in the culture medium

Bioreactor cell culture media collected from samples stimulated with and without cyclic compression for 6 days were either concentrated 5-fold (R_{low} conditions) utilizing the Amicon Ultra® centrifugal filters (UFC501096, Sigma Aldrich), diluted 3-fold (recombinant human BMP2 [rhBMP2] added conditions), or used directly (R_{high} conditions), depending on the experimental condition. The BMP2 concentrations were determined using a human BMP2 ELISA kit (900-M255, PeproTech, Rocky Hill, USA) detecting human BMP2 as well as rhBMP2 produced in *E.coli*. The assay does not exhibit cross reactivity to BMP-3, −5, −6, −7, and − 13 and less than 5% cross reactivity to BMP4 and is therefore highly specific to BMP2. Experiments were conducted according to the manufacturer´s instruction.

2.10 | Measurement of alkaline phosphatase (ALP) activity

Human BMSCs were cultured in 2D for 7 days in OM or normal expansion medium. Thereafter, medium was aspirated, cells were washed once in PBS (37°C) and subsequently in ALP-buffer (37°C; 100 mM sodium chloride, 100 mM Tris [hydroxymethyl] aminomethane, 1 mM magnesium chloride, pH 9). ALP-substrate (4-Nitrophenylphosphat (pNPP) in 1 M Diethanolamine, N4645, Sigma Aldrich) was added and incubated for 10 min at 37°C. Reaction was stopped with 1 M sodium hydroxide. The absorbance was measured in duplicates at 405 nm using a microplate reader (Tecan). The 4-Nitrophenolate concentration, as a measure for the ALP activity, was calculated using the following equation: $c\ [mol/L] = (E\text{-}E_0)/\varepsilon * d$ with E = extinction, E_0 = extinction blank, ε = 18,450 L/mol*cm (molar extinction coefficient), d = 0.329 cm (plate bottom thickness).

2.11 | Cell lysis and western blot analysis

After 60 min of rhBMP2 and recombinant human Noggin (rhNoggin) stimulation, cells seeded in scaffolds were lysed in RIPA buffer (89900, Thermo Fischer Scientific) containing phosphatase (PhosSTOP™, Merck KGaA, Darmstadt, Germany) and protease inhibitors (cOmplete™ Protease Inhibitor Cocktail, Merck KGaA). Samples were incubated for 4 min in the lysis buffer on ice, vortexed, sonicated for 30 sec, and vortexed again. Subsequently, scaffolds were centrifuged through a tip of a 0.5- to 10-µl pipette, thereby collecting the lysate, while the scaffold remained dry inside the tip. Protein lysates were mixed with the 4× loading buffer (928–40004,

TABLE 1 Primer sequences

Protein name	Gene abbrev.	Primer sequences forward (FWD), reverse (REV)	
Human bone morphogenetic protein 2	hBMP2	FWD	CAGCTTCCACCATGAAGAATCT
		REV	AATTTCGAGTTGGCTGTTGC
Human bone morphogenetic protein 4	hBMP4	FWD	CCACGAAGAACATCTGGAGAAC
		REV	ATACGGTGGAAGCCCCTTT
Human bone morphogenetic protein 6	hBMP6	FWD	GCAGACCTTGGTTCACCTTATG
		REV	AGAATGTGTGTCCCCAGCA
Human bone morphogenetic protein 7	hBMP7	FWD	GTCAGGAGTTCGAGACCAGC
		REV	ATCTTGGCTCACTGCAACCT
Collagen 1 (Collagen alpha-2(I) chain)	COL1A2	FWD REV	AGCCGGAGATAGAGGACCAC GGCCAAGTCCAACTCCTTTT
Hypoxanthine phosphoribosyltransferase 1	HPRT1	FWD REV	TATGGACAGGACTGAACGTC TGATGTAATCCAGCAGGTCA
Human inhibitor of DNA binding 1	ID1	FWD REV	GCTGCTCTACGACATGAACG CCAACTGAAGGTCCCTGATG
Noggin	NOG	FWD REV	GTGCAAGCCGTCCAAGTC GCTAGAGGGTGGTGGAACTG
Osteocalcin	BGLAP	FWD REV	TGAGAGCCCTCACACTCCTC CGCCTGGGTCTCTTCACTAC
Osteopontin	SPP1	FWD REV	CACTACCATGAGAATTGCAGTGA CTGCTTTTCCTCAGAACTTCCA
Runt-related transcription factor 2	RUNX2	FWD	CTCCTACCTGAGCCAGATGA
		REV	CGGGGTGTAAGTAAAGGTGG
Transforming growth factor 1	TGFβ1	FWD	GGCCTTTCCTGCTTCTCAT
		REV	GTCCTTGCGGAAGTCAATGT
Transforming growth factor 3	TGFβ3	FWD	ATGAGCACATTGCCAAACAG
		REV	ATTGGGCTGAAAGGTGTGAC
Fibroblast growth factor 2	FGF2	FWD	AGCGGCTGTACTGCAAAAAC
		REV	AGCCAGGTAACGGTTAGCAC
Vascular endothelial growth factor A	VEGF-A	FWD	CAGAAGGAGGAGGGCAGAAT
		REV	CTGCATGGTGATGTTGGACT
Platelet-derived growth factor	PDGF-A	FWD	GCAACACGAGCAGTGTCAAG
		REV	GCTCCTCTAACCTCACCTGG

LI-COR Biosciences, Lincoln, Nebraska, USA), loaded into 4–12% bis-tris polyacrylamide gels (NP0336Box, Thermo Fischer Scientific) and SDS-PAGE was conducted. Thereafter, proteins were transferred on nitrocellulose membranes (741280, Macherey-Nagel GmbH, Düren, Germany) by western blot. Membranes were blocked for 1 hr in TBS (pH 7.6) containing 5% IgG-free albumin (3737.3, Carl Roth GmbH) and incubated in the respective primary antibody overnight at 4°C following the manufacturer's instruction. After washing with TBS-T (pH 7.6, 0.1% tween), membranes were incubated for 2 hr with the secondary antibodies conjugated to fluorescence tags (P/N 925–32211, Li-Cor Biosciences). Proteins were visualized and quantified using the Odyssey Infrared Imager (Li-Cor Biosciences) and the corresponding software. GAPDH served as a loading control to which the proteins of interest were normalized. The following antibodies were used: Phospho-Smad1/5 (Ser463/465; #9516, CST, Danver, USA) and GAPDH (#2118, CST).

2.12 | Statistical analysis

Statistical significance between groups was analyzed using the nonparametric Mann–Whitney Test (two-sided) with Bonferroni correction for multiple comparisons. OriginPro 2015G by OriginLab Corporation was used to prepare all figures including bar charts and box plots as well as the statistical analyses. Bar charts present mean values with standard deviation. Box and whisker plots depict the data minimum, the lower quartile (25%), the median as a horizontal line, the upper quartile (75%), and the maximum of all data points. The mean values are indicated by squares.

3 | RESULTS

3.1 | Cell morphology, proliferation, and oxygen concentration inside scaffolds cultured in the bioreactor

The *in vitro* setup used in this study was specifically designed to resemble the mechanical environment during the early phase of bone healing as it was observed *in vivo*. The utilized scaffolds are characterized by low elastic moduli mimicking the soft tissue matrix in the fracture gap. The bioreactor was used to simulate interfragmentary compression that occur as a consequence of weight bearing in the rage of reported data for external fixation in bone healing in sheep (Klein et al., 2003; Petersen et al., 2012; Schell et al., 2008). At first, to verify that neither bioreactor culture nor cyclic compression have major influences on cell morphology and number after 7 days, confocal imaging was performed and scaffolds cultured in the bioreactor (with and without cyclic compression) were compared with scaffolds cultured in the cell culture incubator (static; Figure 1). Images of hBMSC-seeded scaffolds showed no differences in cell distribution and morphology between different culture time points (1 or 7 days) and conditions (static, bioreactor without cyclic compression, or bioreactor with cyclic compression). Cells were homogeneously distributed throughout the scaffold and showed

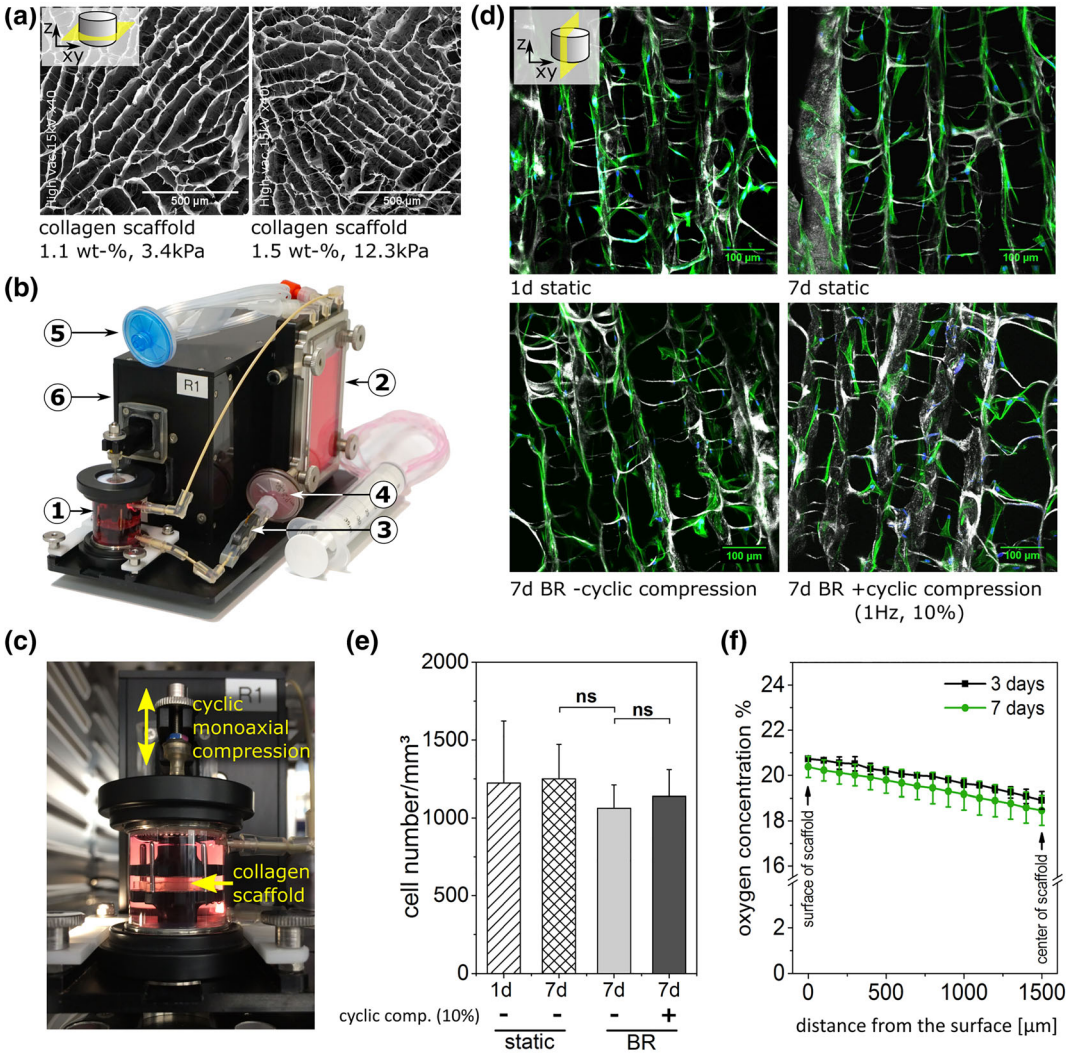

FIGURE 1 **Bioreactor setup validation.** (a) Electron microscopy image of the two scaffold prototypes with collagen solid contents of 1.1 and 1.5 wt-%. (b) Bioreactor consisting of (1) reactor chamber, (2) medium reservoir, (3) micro pump, (4) filter, (5) pressure equalization tube, and (6)the mechanical unit. (c) Close-up of the bioreactor chamber with collagen scaffold inserted. Human BMSCs obtained from three donors were seeded in collagen scaffolds and cultured for 1 or 7 days in well plates under static conditions or in the bioreactor with and without cyclic compression (f = 1 Hz, 10% axial compression). (d) Representative confocal images showing hBMSCs in the collagen scaffold (white), stained with phalloidin (green) and DAPI (blue) to visualize the F-actin fibers and the cell nuclei, respectively. (e) Cell density (cells/mm^3) inside the scaffold as analyzed from confocal image stacks (mean ± SD, three donors, ns = not significant). (f) Concentration of oxygen measured inside the scaffold depending on the distance from the scaffold surface (mean ± SD, n = 2 scaffolds per time point). Statistical significance was tested via Mann–Whitney test (two-sided) with Bonferroni correction [Colour figure can be viewed at wileyonlinelibrary.com]

an elongated morphology in the direction of the scaffold pores (Figure 1d). Analysis of the cell density 7 days after seeding neither showed significant differences between static [1.3(±0.2) × 10^3 cells/mm^3] and bioreactor [1.1(±0.2) × 10^3 cells/mm^3] culture nor an alteration in response to cyclic compression [1.1(±0.2) × 10^3 cells/mm^3]. The comparison with the cell density 1 day after seeding [1.2(±0.4) × 10^3 cells/mm^3] revealed that the cells remained viable but did not proliferate significantly in the microenvironment provided by the scaffold (Figure 1e). The oxygen concentration, measured by opto-chemical microsensors introduced into the sample, showed only a slight decrease from the surface (20.7/20.5%) to the center of the sample (18.9/18.5%) at days 3 and 7 of culture (Figure 1f). This verified that the cells were well-supplied even in the center of the scaffold throughout the duration of this study. Consequently, a potentially improved supply resulting from enhanced fluid flow under cyclic compression could be excluded. Thus, the effects of cyclic compression on gene expression and protein secretion reported in this study could be linked to direct mechanical consequences of cyclic compression. In contrast, supply in other, less open-porous biomaterials might be significantly enhanced by cyclic compression (reduced hypoxia and increased viability) as reported before for cell-seeded fibrin hydrogels (Witt, Duda, Bergmann, & Petersen, 2014).

3.2 | HBMSC migration is reduced by cyclic mechanical compression and osteogenic differentiation

The migration behavior of hBMSCs inside the collagen scaffolds was investigated by an inwards-migration assay where the median migration distance $\widetilde{D}_d$ into the 3D biomaterial was quantified 3 days post-seeding (Figure S1).

In response to cyclic compression, $\widetilde{D}_d$ decreased in a magnitude-dependent way with the strongest reduction of 25% observed for scaffold B (E = 12.3 kPa) and a compression magnitude of 10%. Although the same trend was observed for the softer scaffold A (E = 3.4 kPa), the reduction of cell migration was less pronounced and did not reach statistical significance (Figure 2a). In contrast, the stiffness of the collagen scaffold did not affect migration in the unstimulated control.

Based on these results, we asked whether that the reduction in migration is the consequence of a differentiation process induced by cyclic compression. This was based on, firstly, the previously reported induction of stem cell commitment by loading (reviewed in Delaine-Smith & Reilly, 2011) and, secondly, the observation that undifferentiated MSCs showed faster migration compared with MSCs in a later stage of differentiation (Ichida et al., 2011; Sliogeryte, Thorpe, Lee, Botto, & Knight, 2014). To clarify the influence of differentiation on cell migration inside the biomaterial, the migration distance $\widetilde{D}_d$ of hBMSCs pre-differentiated into the osteogenic lineage was evaluated. HBMSCs of five donors were osteogenically pre-differentiated by treatment with OM in cell culture flasks over 7 days. Subsequently, scaffolds were seeded with these pre-differentiated cells for the 3D migration assay. Induction of osteogenic differentiation after 7 days was confirmed for all donors by an increase in ALP activity (Figure S3). During the 3D migration experiment, undifferentiated and pre-committed hBMSCs were both cultured in migration medium to exclude a direct influence of osteogenic supplements on cell motility. Osteogenic

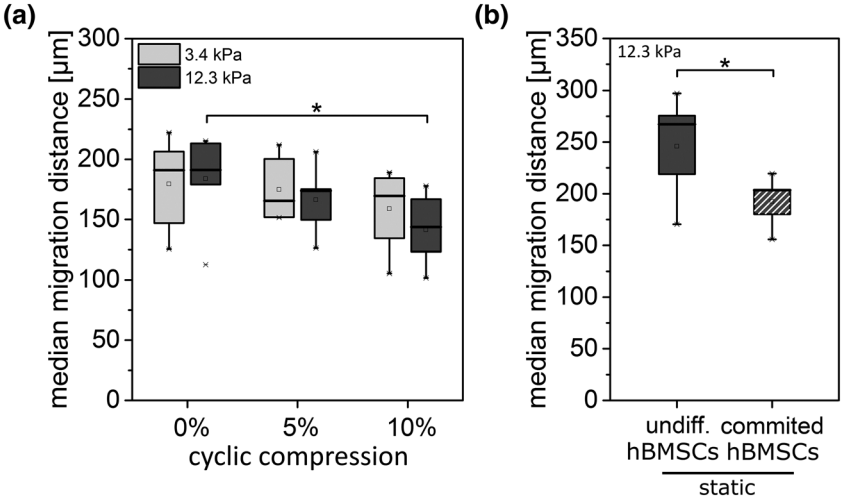

FIGURE 2 Stimulation with cyclic compression and osteogenic medium both reduces hBMSC migration. (a) Human BMSCs seeded in collagen scaffolds of different stiffnesses (scaffold A = 3.4 kPa, scaffold B = 12.3 kPa) were stimulated with 5% or 10% intermittent cyclic mechanical compression or cultured without compression (0%) for 3 days in the bioreactor. Median migration distance was determined for cells from eight different donors for scaffold A and seven for scaffold B. (b) Human BMSCs were treated with osteogenic medium (= committed hBMSCs) in 2D cell culture flasks for 1 week prior to scaffold seeding for the 3D migration experiment. During the migration experiment (3 days), which was performed under static conditions in the cell culture incubator, undifferentiated and committed hBMSCs were incubated in migration medium. Median migration distance was determined for cells of five different donors. Statistical significance was tested via Mann–Whitney test (two-sided) with Bonferroni correction, $^*p \leq 0.05$

commitment of hBMSCs significantly reduced $\widetilde{D}_d$ compared with undifferentiated controls (Figure 2b). Thus, the result supports a putative connection between the cell's migration behavior and differentiation status.

3.3 | Cyclic mechanical compression downregulates the expression of key osteogenic marker genes but upregulates BMP2 expression

To investigate whether the reduction of migration in response to cyclic compression is a result of osteogenic differentiation, the impact of cyclic mechanical compression on the mRNA expression of osteogenic marker genes was quantified by qPCR (Figure 3). Therefore, hBMSCs obtained from eight (scaffold A) or six (scaffold B) different donors were individually seeded in collagen scaffolds and subjected for 6 days to cyclic compression with magnitudes of 5% or 10%. Surprisingly and in contrary to our hypothesis, the median fold-change $\widetilde{FC}$ mRNA expression levels of RUNX2 (early transcription factor for osteogenesis) were reduced in both scaffold types in response to 10% compression, with statistical significance for scaffold A [$\widetilde{FC}(RUNX2)_{scaffA,10\%}$ = 0.8, p = 0.0002; $\widetilde{FC}(RUNX2)_{scaffB,10\%}$ = 0.81]. Cyclic compression of 5% significantly decreased the RUNX2 expression in scaffold A [$\widetilde{FC}(RUNX2)_{scaffA,5\%}$ = 0.7, p = 0.01], whereas no change was visible in scaffold B [$\widetilde{FC}(RUNX2)_{scaffB,5\%}$ = 0.98]. The median mRNA expressions of osteocalcin (BGLAP) and collagen type 1 α 2 (COL1A2) were also decreased for both scaffold stiffnesses and loading magnitudes in comparison with the uncompressed controls, reaching statistical significance for BGLAP in response to 10% compression in scaffold B [$\widetilde{FC}(OC)_{scaffB,10\%}$ = 0.56, p = 0.0007].

The median expression of osteopontin (SPP1) under 5% cyclic compression remained unchanged, whereas 10% compression significantly increased the SPP1 expression for the softer scaffolds [$\widetilde{FC}(OP)_{scaffA,10\%}$ = 2.24, p = 0.01] but not for the stiffer. Interestingly, mechanical stimulation induced an upregulation of BMP2 mRNA expression in scaffold B at 5 and 10% and in scaffold A at 10% compression. Statistical significance was reached at 10% compression in scaffold B [$\widetilde{FC}(BMP2)_{scaffB,10\%}$ = 1.47, p = 0.02].

In summary, we found a clear downregulation of important osteogenic marker genes, especially of RUNX2, in response to cyclic

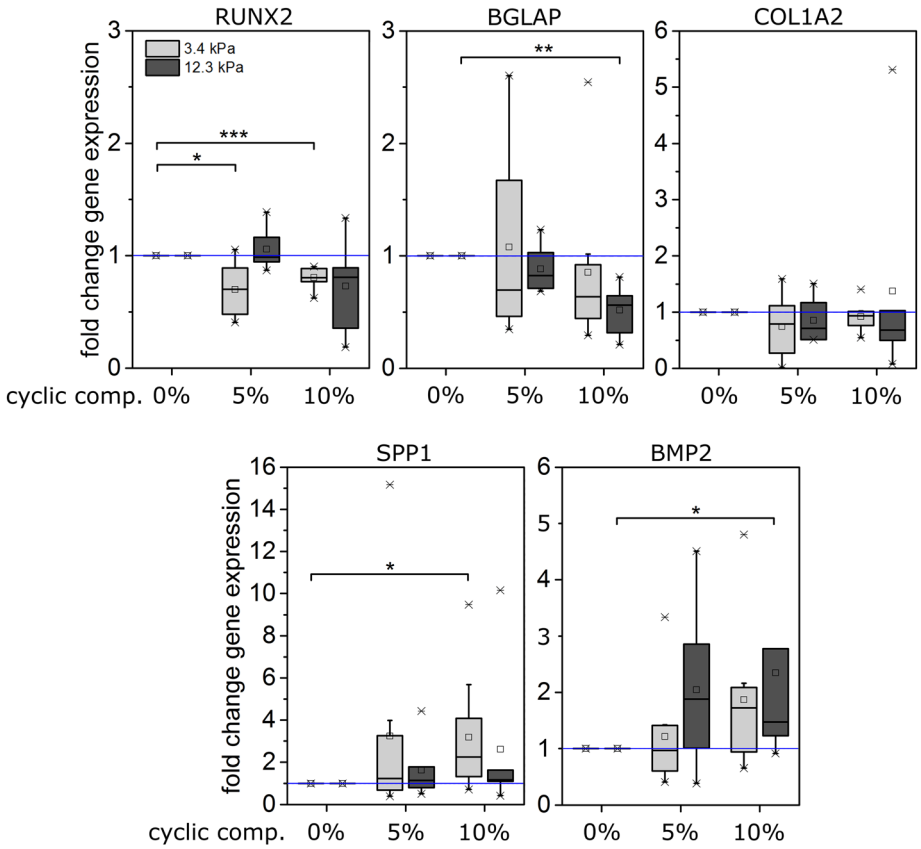

FIGURE 3 **Cyclic compression downregulates the expression of key osteogenic marker genes but upregulates BMP2 expression.** Human BMSCs obtained from various donors were seeded in collagen scaffolds of 3.4 kPa (n = 8 donors)/12.3 kPa (n = 6 donors) stiffness, respectively. Scaffolds were cultured for 6 days in the bioreactor under 5% or 10% intermittent cyclic compression or were left unstimulated (0%). mRNA expression was analyzed by qPCR. Fold change expressions to the 0% control group of the respective scaffold type are depicted in box and whisker plots. Statistical significance was tested via Mann–Whitney test (two-sided) with Bonferroni correction, *$p \leq 0.05$, **$p \leq 0.01$, ***$p \leq 0.001$ [Colour figure can be viewed at wileyonlinelibrary.com]

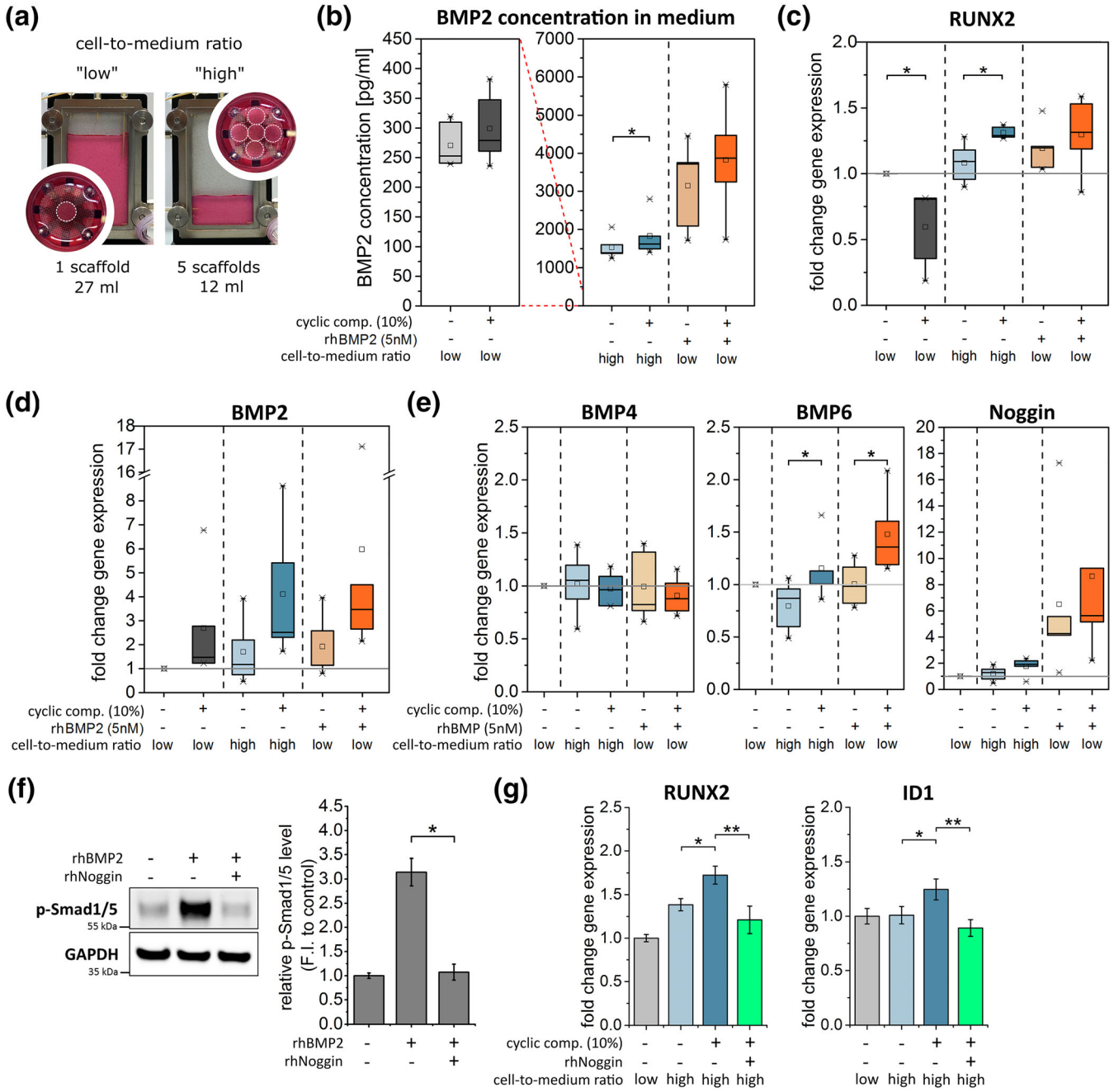

FIGURE 4 **Cyclic compression only increases RUNX2 expression, if rhBMP2 is added or an enrichment of cell-secreted BMP2 in the cell culture medium was permitted.** (a) Data was obtained from three different experimental conditions: (1) Human BMSCs were seeded in collagen scaffolds (12.3 kPa) and cultured with or without cyclic compression (f = 1 Hz, ε = 10%) for 6 days. (2) hBMSCs were additionally stimulated with recombinant human BMP2 (rhBMP2, 5 nM) added at the 4th day of cultivation (+ rhBMP2). (3) The cell number was increased 5 times and the medium volume was reduced from 27 ml to 12 ml ("high cell-to-medium ratio"). (b) Human BMP2 ELISA of collected bioreactor media from all loading experiments were conducted. The relative gene expressions of (c) RUNX2, (d) BMP2, (e) BMP4, BMP6, and Noggin (n = 5 hBMSC donors). (f) Validation of rhNoggin efficiency by western blot analysis of p-Smad1/5 level after 60 min of rhBMP2 stimulation. Phosphorylation was normalized to GAPDH (n = 3, one donor). (g) Scaffolds were cultured under high cell-to-medium ratio with or without 10% cyclic compression and with or without rhNoggin stimulation (100 ng/ml, added at Days 1, 3, and 5), and RUNX2 and ID1 expression were analyzed. Gene expressions were analyzed by qPCR. HPRT1 was used as the reference gene, and expressions were normalized to the untreated control (low cell-to-medium-ratio, without cyclic compression; $n \geq 4$ for one donor). Statistical significance was tested via Mann–Whitney test (two-sided) with Bonferroni correction, $^{*}p \leq 0.05$, $^{**}p \leq 0.01$ [Colour figure can be viewed at wileyonlinelibrary.com]

mechanical compression. However, BMP2, a growth factor known to be a potent inducer of osteogenic differentation, was clearly upregulated under 10% cyclic compression.

3.4 | Limited biochemical conditioning of the culture medium during bioreactor culture

To study whether the observed increase in BMP2 gene expression resulted in an increased protein expression and secretion, BMP2 protein concentrations $\beta(BMP2)$ were analyzed using an enzyme-linked immunosorbent assay (ELISA) specific for human BMP2 (Figure 4b, left). In agreement with the expression data, a slight increase of BMP2 was detected in culture media of samples stimulated with 10% compression $\left[\widetilde{\beta}(BMP2)_{0\%} = 252 \text{ pg/ml}, \widetilde{\beta}(BMP2)_{10\%} = 280 \text{ pg/ml}\right]$. The detected BMP2-concentrations were in general very low and, according to Katagiri (Katagiri et al., 1994), not capable to stimulate an osteogenic response. This could be explained by the comparably low cell number in respect to the large medium volume (1.5×10^5 cells/27 ml medium = 5.6×10^3 cells/ml) in the bioreactors. The cell-to-medium ratio in the bioreactor was approximately 9 times lower compared with typical 2D culture conditions (5×10^4 cells/ml). Therefore, the gene expression data was obtained from bioreactor experiments (Figure 3) under a strong dilution of secreted proteins. The observed gene regulations thus represented consequences of cyclic compression without relevant contributions of autocrine biochemical stimulation.

3.5 | A higher cell-to-medium ratio significantly increased BMP2 concentrations in the culture medium

With the goal to promote medium conditioning and autocrine BMP2 signaling during bioreactor cultivation (6 days), the ratio between cell number and medium volume was increased in subsequent experiments. The number of scaffolds per bioreactor was increased from one to five, and the medium volume was reduced from 27 ml to 12 ml (minimal filling volume of the bioreactor), resulting in an increase in cell-to-medium ratio from $R_{low} = 0.56 \times 10^4$ to $R_{high} = 6.25 \times 10^4$ cells/ml. Additionally, we conducted separate control experiments where 5 nM (135 ng/ml) rhBMP2 was added at Day 4 of bioreactor cultivation to compare the impact of medium conditioning with direct BMP2 stimulation. These experiments were conducted using the 12.3 kPa scaffold and the five donors of the six that showed a consistent down-regulation in RUNX2 expression upon cyclic compression. As expected, the increase in cell-to-medium ratio enabled a significant 5.5-fold increase of BMP2 concentration ($p = 0.004$) in the cell culture medium from $\widetilde{\beta}(\text{BMP2})_{\text{Rlow,−cyclic comp.}} = 252$ pg/ml to $\widetilde{\beta}(\text{BMP2})_{\text{Rhigh,−cyclic comp.}} = 1395$ pg/ml $\widetilde{\beta}(\text{BMP2})_{\text{Rlow,−load}}\widetilde{\beta}(\text{BMP2})_{\text{Rhigh,−load}}$ (Figure 4b, light grey vs. light blue box). In response to cyclic compression, the BMP2 concentration increased slightly but significantly (Figure 4b, dark blue vs. light blue box, $\left[\widetilde{\beta}(\text{BMP2})_{\text{Rhigh,+cyclic comp.}} = 1623 \text{ pg/ml}\right]$). This is in agreement with the observed increase in BMP2 gene expression under load, strengthening the assumption that cyclic compression triggers a positive feedback loop for BMP2.

Next, we analyzed the concentration of BMP2 in the conditioned media collected from bioreactors that were supplemented with rhBMP2. Also here, mechanical loading increased BMP2 concentration slightly but nonsignificantly (Figure 4b, dark vs. light orange box) $\widetilde{\beta}(\text{BMP2})_{0\%}$. It has to be mentioned that the detected BMP2 concentrations were overall very low compared with the initially added amount of rhBMP2 (135 ng/ml). To understand this discrepancy, we analyzed the BMP2 stability in the bioreactor. Therefore, 135 ng/ml rhBMP2 was added to the bioreactor experiment (conducted without cells), and medium samples were collected after 30 min and at Days 1, 3, 5, and 7 (supplementary Figure 5). Already after one day, BMP2 concentration decreased to about one third and declined further during culture. Together, this indicated that BMP2 stability is transient under cell culture conditions.

3.6 | Mechanical loading enhances RUNX2 mRNA expression only in a BMP-enriched environment

Signaling initiated by BMP2 directly stimulates the expression of RUNX2 and balances its transcriptional activity (Nishimura, Hata, Matsubara, Wakabayashi, & Yoneda, 2012; Yang et al., 2016). Therefore, BMP2 is an important trigger for early osteogenic responses. Consequently, the observed upregulation of BMP2 expression in response to mechanical loading led us to the assumption that hBMSCs would trigger themselves toward osteogenic differentiation (enhance RUNX2 expression) in response to cyclic loading under increased cell-to-medium ratio R_{high}.

Strikingly, under R_{high} conditions, RUNX2 expression was significantly upregulated in response to cyclic compression in comparison with the uncompressed control (Figure 4c, dark blue box, $[\widetilde{FC}(\text{RUNX2})_{\text{Rhigh,+cyclic comp.}} = 1.3, p = 0.036]$). This finding stands in strong contrast to the regulation of RUNX2 in response to cyclic loading under R_{low} conditions in the original setup (Figure 4c, gray box, $[\widetilde{FC}(\text{RUNX2})_{\text{Rlow,+cyclic comp.}} = 0.8, p = 0.021]$). Additionally, RUNX2 expression under rhBMP2 supplementation was also further enhanced by cyclic compression (Figure 4c, dark orange box $[\widetilde{FC}(\text{RUNX2})_{\text{+rhBMP2,+cyclic comp.}} = 1.32]$). This indicated that BMP2 is capable to alter the cell's gene expression response to mechanical loading. Moreover, in response to (i) the increase of the cell-to-medium ratio from R_{low} to R_{high} and (ii) the supplementation of rhBMP2, concurrent cyclic compression further enhanced the expression of BMP2, suggesting a positive feedback regulation by biochemical self-stimulation (Figure 4d, dark blue and dark orange box, $[\widetilde{FC}(\text{BMP2})_{\text{Rhigh,+cyclic comp.}} = 2.5, \widetilde{FC}(\text{BMP2})_{\text{+BMP2,+cyclic comp.}} = 3.5]$).

To investigate the involvement of possible further feedback components, we also analyzed the expression of BMP4, −6, and − 7, as well as the expression of the BMP antagonist Noggin (Figure 4e). Expression of BMP4 was not affected by neither condition, and BMP7 transcription was not detected. BMP6 expression, instead, was found to be sensitive to cyclic compression. Under rhBMP2

supplementation, loading induced a 1.4-fold increase in BMP6 transcription, whereas in the R_{high} condition, only a slight 1.1-fold increase was detected. Taking into account the observed mechanosensitivity of BMP6 expression, a potential contribution to the RUNX2 regulation cannot be excluded. However, in comparison with the according changes in BMP2 expression, the contribution of regulations in BMP6-expression is regarded to be low. Noggin expression strongly increased by 4.3-fold in response to rhBMP2 treatment and increased further to 5.6-fold by cyclic compression. Under high cell-to-medium ratio, cyclic compression increased Noggin transcription by 1.9-fold. The regulation of Noggin expression under both conditions is in line with the increased BMP2 expression and medium concentration. Noggin inhibits BMP2, −4, −7, and − 14 from binding to the BMP receptor. BMP6 however is more resistant to noggin inhibition (Krause, Guzman, & Knaus, 2011). Additionally, the expressions of transforming growth factor beta-1 and 3 (TGFβ1 and β3), fibroblast growth factor-2 (FGF2), platelet-derived growth factor-A (PDGF), and vascular endothelial growth factor-A (VEGF-A) that are of relevance in osteogenic differentiation were analyzed (Figure S4). FGF-2 and PDGF-A expressions were not regulated by any of the treatments. TGFβ1, TGFβ3, and VEGF-A expressions were increased in response to cyclic compression under rhBMP2 stimulation. However, in the high cell-to-medium ratio group, only the expression of TGFβ3 was increased by 1.35-fold upon cyclic compression, and the others were not consistently regulated. No statistical significant differences could be found. Therefore, in comparison with the 2.5-fold change in BMP2 expression under cyclic compression, only modest changes were detected.

To finally verify that the load-induced increase in RUNX2 expression is mediated by BMP2, in the next experiment, BMP2 was depleted from the system by rhNoggin. At first, the effect of the rhNoggin on BMP signaling was validated in a separate experiment by western blot analysis investigating the phosphorylation of the transcription factor Smad1/5 (Figure 4f). Although Smad1/5 phosphorylation was increased by 3-fold in response to 5 nM rhBMP2, no increase was detected if cells were treated with rhBMP2 and rhNoggin (12 nM). Next, for the proof of concept experiment, one hBMSC donor representing the group was selected. Cells were cultured under R_{high} conditions with or without cyclic compression and rhNoggin (100 ng/ml equals 2.2 nM), which was added at Days 1, 3, and 5. Again, RUNX2 expression was significantly upregulated in response to cyclic compression; however rhNoggin treatment abolished the effect of compression completely. Furthermore, the expression of ID1 (inhibitor of DNA binding 1), a commonly used BMP target gene, was investigated. Under R_{high} conditions, ID1 expression was significantly induced by cyclic compression and significantly reduced by rhNoggin treatment (Figure 4g).

Taken together, the results show that cyclic compression strongly downregulated the expression of RUNX2 when the cell-to-medium ratio was low and BMP self-conditioning was impeded by dilution. However, after increasing the ratio, cyclic compression significantly upregulated RUNX2 expression. Both observation, (i) that rhBMP2 stimulation led to a very similar result as the increase in cell-to-medium ratio and (ii) that the load-induced effect on RUNX2 and ID1 expressions were abolished by rhNoggin treatment, verify the role of BMP2 as the relevant mechanoregulated signaling factor controlling RUNX2 and consequently osteogenesis.

4 | DISCUSSION

4.1 | Mimicking the mechanical loading conditions during the early phase of bone healing

The biomaterial used in this study was made from fibrillar collagen, a component of the extracellular matrix that is a relevant cell substrate throughout the bone healing process (Petersen et al., 2018). The macroporous architecture assures three-dimensional cell morphology and provides enhanced nutrient and oxygen supply for the cells even in the center for the scaffold. Collagen crosslinking during production protects the scaffolds from fast enzymatic degradation. Both, collagen crosslinking and its elastic deformation behavior allowed repetitive compression without major shape-changes even over long periods of time (Brauer et al., 2019; Petersen et al., 2018). By changing the solid content, the wall stiffness was tuned without affecting the pore architecture (Figure 1a). As the stiffness of the substrate that cells adhere to is known to be an important regulator influencing cellular behavior (Engler, Sen, Sweeney, & Discher, 2006), scaffolds with bulk stiffnesses of 3.4 kPa and 12.3 kPa were used in this study. The utilized scaffolds are characterized by low elastic moduli mimicking the physical environment in the fracture gap early after bone injury where a soft tissue matrix is present within the fracture gap.

The early healing phase is especially sensitive to mechanical signals and is believed to lay the ground for the entire repair process. Indeed, allowing a limited interfragmentary movement in the early phase was shown to enhance fracture healing in a sheep model (Klein et al., 2003). Axial interfragmentary movement was reported to be the main loading regime in animal osteotomy models with an external fixator (Bottlang & Feist, 2011). Interfragmentary compression that occurs as a consequence of weight bearing in experimental bone healing studies was reported to range between 10 and 33% (Klein et al., 2003; Schell et al., 2008) and 2 and 20% (Claes & Heigele, 1999; Klosterhoff et al., 2017) of the fracture gap for sheep and rat osteotomies, respectively. According to the reported *in vivo* data and in agreement with previous studies investigating the impact of mechanical loading on cell differentiation (Jagodzinski et al., 2008; Liu et al., 2012; Michalopoulos et al., 2012; Sittichokechaiwut, Edwards, & Scutt, a M., & Reilly, G. C., 2010), strain regimes of 5 and 10% were selected. To mimic the load pattern during human locomotion (Morlock et al., 2001), a sinusoidal compression with a frequency of f = 1 Hz was applied in this study using mechanobioreactors. In summary, the loading parameters used in this study were chosen to represent regimes occurring *in vivo*, more specifically, to mimic the mechanical environment in the early fracture gap.

4.2 | Cell migration is downregulated by mechanical loading independent of osteogenic differentiation

In this study, a significant reduction of the migration capacity of hBMSCs was observed in response to the application of 10% cyclic compressive loading. Previous studies have already shown that cell migration is influenced by external mechanical forces. Contrary results were reported depending on the cell type and experimental system used. A reduction of the migration capacity in response to cyclic stretch or compression has been demonstrated for alveolar epithelial cells (Desai, Chapman, & Waters, 2008) and rat bone marrow MSCs, respectively (Ode et al., 2011). However, a stimulating effect of cyclic mechanical stretch was seen for osteoblasts (Bhatt et al., 2007) and fibroblasts (Raeber, Lutolf, & Hubbell, 2008). So far, migration has been studied mainly in two dimensional environments (Bhatt et al., 2007; Desai et al., 2008; Li, Wernig, Hu, & Xu, 2003). A direct comparison with these studies is difficult because integrin expression pattern may be essentially affected by the dimensionality of the environment (Hong & Stegemann, 2008). In this regard, the present work is compared with the study by Ode et al. (2011) in which rat MSCs seeded in a 3D fibrin gel matrix were subjected to cyclic compression. In line with the data presented here, the migration capacity was significantly reduced by about 40% after the application of 20% compressive strain (f = 1 Hz, 72 hr). However, for the evaluation of MSC migration, the cells had to be removed from the 3D fibrin matrix and transferred into 2D transwell plates. In the present study, a cell migration assay was used that allows to study the direct impact of cyclic compression on cell migration in a 3D environment, mimicking the *in vivo* situation.

Interestingly, the strongest reduction of the migration distance in response to 10% mechanical strain could be seen in the stiffer scaffold B (25% reduction in scaffold B vs. 12% reduction in scaffold A). Because the median migration distance of uncompressed control hBMSCs was found to be independent of scaffold stiffness, this indicated a stiffness-dependent cell response to load. Cells on stiffer substrates may sense extrinsic mechanical stimulation differently because, in stiffer scaffolds, the influence of the cell's own forces on the extrinsically induced wall deformation is limited and the signal might be transmitted more directly to the cells. However, for a deeper understanding of the force-interplay and the molecular consequences, more mechanistic investigations are needed.

Based on our findings it can be concluded that the migration of hBMSCs is strongly affected by *in vivo*-motivated mechanical loading regimes. An accumulation of attracted bone marrow MSCs at locations of increased mechanical strain could represent a conceivable physiological mechanism in healing of bone fractures and bone defects. Previous *in vivo* and *in vitro* studies reported that mechanical loading induces the differentiation of osteoprogenitors into osteoblasts (Jagodzinski et al., 2008; Michalopoulos et al., 2012; Shin Kang et al., 2013; Sittichokechaiwut et al., 2010; Turner, Owan, Alvey, Hulman, & Hock, 1998). Concerning our finding that hBMSC migration is reduced in response to cyclic compression, this led to the assumption that a reduction in migration is caused or at least accompanied by an onset of osteogenic differentiation. This was initially supported by our observation that the migration capacity of hBMSCs was clearly reduced after induction of osteogenic differentiation using OM. Also, previous studies have found reduced migration with advancing differentiation (Ichida et al., 2011; Sliogeryte et al., 2014). However, the fact that cyclic compression failed to induce osteogenic differentiation in our study indicated that loading and differentiation interfered with hBMSC migration independent of each other.

4.3 | Towards a deeper understanding how cyclic compression influences osteogenic differentiation

To study the impact of mechanical loading on cell behavior, multiple different experimental setups and loading devices were developed. Here, only studies with 3D cell cultures and comparable mechanical loading regimes (cyclic biomaterial compression) are discussed.

RUNX2 (Cbfa 1), a member of the RUNT domain gene family, is an indispensable transcription factor for osteoblast differentiation (Ducy, Zhang, Geoffroy, Ridall, & Karsenty, 1997). In our study, the expression of RUNX2 in hBMSCs was found to be downregulated upon cyclic compressive loading (Figure 3). This observation stands in contrast to previous reports in which comparable experimental setups were used (Jagodzinski et al., 2008;Michalopoulos et al., 2012 ; Shin Kang et al., 2013 ; Sittichokechaiwut et al., 2010). It is known that RUNX2 regulates the expression of osteoblast-specific genes such as collagen type 1, bone sialoprotein, osteocalcin, and RUNX2 itself (Franceschi & Xiao, 2003). Thus, the downregulation of COL1A2, which encodes the pro-alpha2 chain of type I collagen and osteocalcin that we observed in our study is most likely a consequence of the downregulation of RUNX2.

Only one study was identified that reported an inhibitory effect of mechanical stimulation on the RUNX2 expression and, consequently, on other osteogenic markers. In this study, continuous application of mechanical loading over up to 10 days might be responsible for the negative impact (Shi et al., 2011). However, this can be excluded as an explanation in our study because, here, only intermittent loading (repeated cycles of 3-hr cyclic compression and 5-hr break) was applied.

In contrast to RUNX2, COL1A2, and osteocalcin, we found a significant upregulation of osteopontin mRNA expression in response to 10% compression in the softer scaffold A (E = 3.4 kPa). A possible explanation for this discrepancy is that osteopontin expression is regulated by an alternative mechanism independent of RUNX2. The expression of osteopontin was previously found to be sensitive to mechanical stimulations (Klein-Nulend, Roelofsen, Semeins, Bronckers, & Burger, 1997; Sittichokechaiwut et al., 2010). Osteopontin is an abundant noncollagenous protein in the extracellular matrix of bones and serves as a cell attachment point mediated through integrin binding (Toma, Ashkar, Gray, Schaffer, & Gerstenfeld, 1997). It is conceivable that hBMSCs establish stronger attachments to their substrate in response to the cyclic deformation of the walls by increased osteopontin secretion.

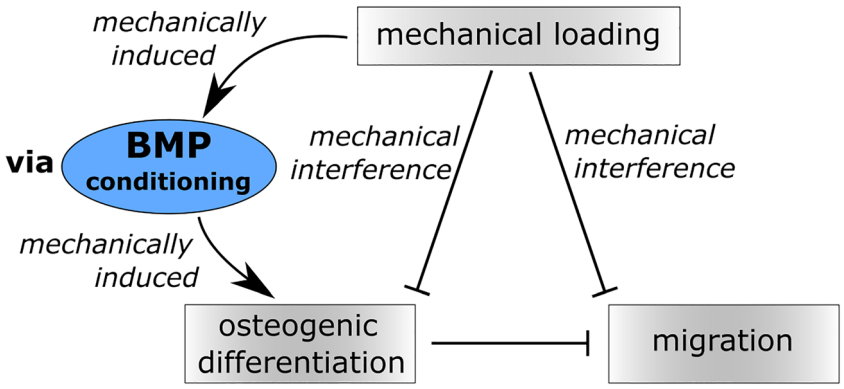

FIGURE 5 Schematic summary for the interconnection between mechanics, differentiation, and migration. Findings of this study indicate that mechanical loading (cyclic compression) and the commitment to the osteogenic lineage both reduces the migration capacity of primary hBMSC. However, the decreased migration under load does not correlate with enhanced differentiation. In this study, mechanical stimulation alone did not promote the osteogenic differentiation but enhanced the expression of BMP2. It is proposed that mechanical loading is able to promote osteogenic differentiation via autocrine signaling through BMP2 [Colour figure can be viewed at wileyonlinelibrary.com]

In summary, aside from osteopontin, all investigated osteogenic marker genes were found to be downregulated in response to cyclic compression. This surprising finding contradicts the majority of literature on this topic as well as our original study hypothesis. A reason for the discrepancy may be found in the specific experimental conditions. In comparison with others, we can exclude previously reported indirect effects of mechanical loading on oxygen concentration and nutrient supply inside the biomaterial due to the chosen macroporous architecture (Witt et al., 2014). A further major difference is the low total cell number in relation to the volume of cell culture medium in the bioreactor (1.5×10^5 cells/27 ml medium) compared with the cultivation of 3D cell seeded constructs in well plates with low medium volume (Michalopoulos et al., 2012; Shin Kang et al., 2013; Sittichokechaiwut et al., 2010). This, in combination with the small but decisive fluid flow in the bioreactor, leads to a strong dilution of signaling proteins secreted by the cells and hinder autocrine biochemical self-stimulation.

4.4 | Cyclic compression possess an osteoinductive potential only in a BMP-enriched environment

As an indicator for an osteogenic response to cyclic compressive loading, and in contrast to the osteogenic genes mentioned above, BMP2 expression and secretion were found to be upregulated. In previous studies, BMP2 was already described to be a target of mechanotransduction. An upregulation in response to mechanical loading was reported by several research groups (Rui et al., 2011; Sumanasinghe, Bernacki, & Loboa, 2006). The growth factor BMP2 is known to be an indispensable player during bone repair (Tsuji et al., 2006), and its administration leads to bone defect healing (Wulsten et al., 2011). In fact, BMP signaling regulates the transcription of RUNX2 through the activation of the Smad transcription factors (Nishimura et al., 2012). Based on this connection, we hypothesized that cyclic compression does not induce osteogenic differentiation per se but only in presence of BMP.

The addition of rhBMP2 in combination with cyclic compression caused a strong enhancement of RUNX2 and BMP2 gene expression. This observation is remarkable because, in the absence of rhBMP2, cyclic compression suppressed the transcription of RUNX2 mRNA. Hence, it indicates that BMP2 is capable to alter the cell's gene expression response to cyclic compression. Strikingly, after increasing the cell-to-medium ratio in the bioreactor experiments, the fold change expression of RUNX2 was significantly increased in response to 10% cyclic compression even in the absence of an additional rhBMP2 stimulus. The changed culture conditions enabled a significant enrichment of BMP2 in the culture medium, confirmed by ELISA quantification (Figure 4b). Cyclic compression further increased BMP2 expression and secretion pointing to an autocrine BMP-mediated increase of RUNX2 expression. The rhNoggin treatment verified the importance of cell-secreted BMP2 in inducing RUNX2 expression under cyclic compression. That rhNoggin treatment did not fully recapitulate R_{low} conditions under which RUNX2 expression was downregulated could have two reasons, either the rhNoggin concentration was not sufficient to fully inhibit BMP2 signaling or a BMP independent mechanism is additionally acting under R_{high} conditions. A BMP2-mediated induction of osteogenic differentiation under cyclic compressive load was previously postulated (Rui et al., 2011; Wang et al., 2010). Rui et al. (2011) correlated an upregulation of BMP2 expression under loading conditions to an increased expression of either RUNX2 or ALP in rat tendon derived stem cells. However, the hypothesis was not proven by the exclusion of BMP2 from their systems as it was done here by the dilution effect (in R_{low} condition) and the addition of rhNoggin (in R_{high} condition). Wang et al. (2010) instead showed in a 2D setting using the MC3T3-E1 cell line that Noggin treatment abolished the ALP expression induced by mechanical loading (four-point bending device), thereby demonstrating the role of BMP in this context. Our findings highlight the physiological relevance of load-induced effects for cell differentiation processes in a 3D bone healing context because we utilized primary human bone marrow-derived MSCs from multiple

donors. We found that the increase of BMP expression in response to cyclic compression contributes to a positive feedback loop enhancing osteogenesis. In addition, cyclic compression not only increases the expression of but also the sensitivity for BMP2. We previously showed in human fetal osteoblasts (Kopf et al., 2012) and in hBMSCs (data not shown) that cyclic compression enhances BMP2-signaling events under concurrent BMP2 stimulation. These two mechanoregulated processes; increased expression of and increased sensitivity for BMP2 seem to contribute jointly to the osteogenic commitment of hBMSCs under cyclic mechanical compression. Further investigations of the regulation of BMP downstream targets under cyclic compression are necessary.

5 | CONCLUSION

In summary (Figure 5), this study showed that cyclic compressive loading per se does not trigger osteogenic differentiation but causes a downregulation of RUNX2 and osteocalcin. Osteogenic differentiation, indicated by increased RUNX2 expression, was only promoted by cyclic compression, if an enrichment of secreted factors including BMP2 in the cell culture medium and resulting biochemical self-stimulation was permitted. This observation provides evidence that mechanical stimulation induces osteogenic differentiation via a mechanoregulated autocrine feedback mechanism.

The impairment of cell migration in response to cyclic compression was not coupled to the onset of osteogenic differentiation as hypothesized. Rather, mechanical stimulation itself interfered with hBMSC migration. Translated into a bone healing scenario, our findings indicate that MSCs migrate into the early fracture hematoma where increased mechanical straining causes them to slow down and to enhance the secretion of BMP2. Together with the increased responsiveness to BMP2 under cyclic compression, osteogenic genes are upregulated triggering differentiation. These findings motivate a more detailed investigation of the complex interplay between BMP signaling and mechanobiology to understand its full biological relevance for bone regeneration.

ACKNOWLEDGEMENT

This study was supported by the RMS Foundation (Robert Mathys Stiftung), Switzerland, funding number E11_0009: 3D scaff-stiff, and the German Research Foundation (DFG), grant no. PE 1802/1-1 within the research group FOR 2165. We would like to thank the Berlin-Brandenburg Center for Regenerative Therapies (BCRT) Core Unit "Cell Harvesting" for providing human mesenchymal stromal cells for this study. Contribution for the PhD student was made possible by DFG funding through the Berlin-Brandenburg School for Regenerative Therapies GSC 203.

CONFLICT OF INTEREST

The authors declare that no competing interests exist.

ETHICAL STATEMENT

The use of primary human bone marrow mesenchymal stromal cells was approved by the ethics committee of the Charité–Universitätsmedizin Berlin, and donors' written informed consent was given.

ORCID

Sophie Schreivogel https://orcid.org/0000-0002-2302-8351
Georg N. Duda https://orcid.org/0000-0001-7605-3908
Ansgar Petersen https://orcid.org/0000-0002-3075-4300

REFERENCES

Betts, D. C., & Müller, R. (2014). Mechanical regulation of bone regeneration: Theories, models, and experiments. *Frontiers in Endocrinology*, *5*, 211. https://doi.org/10.3389/fendo.2014.00211

Bhatt, K. a., Chang, E. I., Warren, S. M., Lin, S., Bastidas, N., Ghali, S., … Gurtner, G. C. (2007). Uniaxial mechanical strain: An in vitro correlate to distraction osteogenesis. *Journal of Surgical Research*, *143*(2), 329–336. https://doi.org/10.1016/j.jss.2007.01.023

Bottlang, M., & Feist, F. (2011). Biomechanics of far cortical locking. *Journal of Orthopaedic Trauma*, *25*, S21–S28. https://doi.org/10.1097/BOT.0b013e318207885b

Brauer, E., Lippens, E., Klein, O., Nebrich, G., Schreivogel, S., Korus, G., … Petersen, A. (2019). Collagen fibrils mechanically contribute to tissue contraction in an in vitro wound healing scenario. *Advanced Science*, *6*(9), 1801780. https://doi.org/10.1002/advs.201801780

Claes, L., & Heigele, C. (1999). Magnitudes of local stress and strain along bony surfaces predict the course and type of fracture healing. *Journal of Biomechanics*, *32*(3), 255–266. https://doi.org/10.1016/S0021-9290(98)00153-5

Delaine-Smith, R. M., & Reilly, G. C. (2011). *The effects of mechanical loading on mesenchymal stem cell differentiation and matrix production. Stem Ccell Rregulators* (1st ed., Vol. 87). Sheffield, United Kingdom: Elsevier Inc. https://doi.org/10.1016/B978-0-12-386015-6.00039-1

Desai, L. P., Chapman, K. E., & Waters, C. M. (2008). Mechanical stretch decreases migration of alveolar epithelial cells through mechanisms involving Rac1 and Tiam1. *American Journal of Physiology. Lung Cellular and Molecular Physiology*, *295*(5), L958–L965. https://doi.org/10.1152/ajplung.90218.2008

Ducy, P., Zhang, R., Geoffroy, V., Ridall, A. L., & Karsenty, G. (1997). Osf2/Cbfa1: A transcriptional activator of osteoblast differentiation. *Cell*, *89*(5), 747–754. Retrieved from. http://www.ncbi.nlm.nih.gov/pubmed/9182762

Duda, G. N., Mandruzzato, F., Heller, M., Goldhahn, J., Moser, R., Hehli, M., … Haas, N. P. (2001). Mechanical boundary conditions of fracture healing: Borderline indications in the treatment of unreamed tibial nailing. *Journal of Biomechanics*, *34*(5), 639–650. Retrieved from. http://www.ncbi.nlm.nih.gov/pubmed/11311705, https://doi.org/10.1016/S0021-9290(00)00237-2

Engler, A. J., Sen, S., Sweeney, H. L., & Discher, D. E. (2006). Matrix elasticity directs stem cell lineage specification. *Cell*, *126*(4), 677–689. https://doi.org/10.1016/j.cell.2006.06.044

Epari, D. R., Taylor, W. R., Heller, M. O., & Duda, G. N. (2006). Mechanical conditions in the initial phase of bone healing. *Clinical Biomechanics (Bristol, Avon)*, *21*(6), 646–655. https://doi.org/10.1016/j.clinbiomech.2006.01.003

Franceschi, R. T., & Xiao, G. (2003). Regulation of the osteoblast-specific transcription factor, Runx2: Responsiveness to multiple signal

transduction pathways. *Journal of Cellular Biochemistry*, *88*(3), 446–454. https://doi.org/10.1002/jcb.10369

Gerstenfeld, L. C., Cullinane, D. M., Barnes, G. L., Graves, D. T., & Einhorn, T. A. (2003). Fracture healing as a post-natal developmental process: Molecular, spatial, and temporal aspects of its regulation. *Journal of Cellular Biochemistry*, *88*(5), 873–884. https://doi.org/10.1002/jcb.10435

Goodship, A. E., Cunningham, J. L., & Kenwright, J. (1998). Strain rate and timing of stimulation in mechanical modulation of fracture healing. *Clinical Orthopaedics and Related Research*, (355 Suppl), S105–S115. Retrieved from. http://www.ncbi.nlm.nih.gov/pubmed/9917631

Herrera, A., Hellwig, J., Leemhuis, H., von Klitzing, R., Heschel, I., Duda, G. N., & Petersen, A. (2019). From macroscopic mechanics to cell-effective stiffness within highly aligned macroporous collagen scaffolds. *Materials Science and Engineering: C*, *103*, 109760. https://doi.org/10.1016/J.MSEC.2019.109760

Hong, H., & Stegemann, J. P. (2008). 2D and 3D collagen and fibrin biopolymers promote specific ECM and integrin gene expression by vascular smooth muscle cells. *Journal of Biomaterials Science*. Polymer Edition, *19*(10), 1279–1293. https://doi.org/10.1163/156856208786052380

Ichida, M., Yui, Y., Yoshioka, K., Tanaka, T., Wakamatsu, T., Yoshikawa, H., & Itoh, K. (2011). Changes in cell migration of mesenchymal cells during osteogenic differentiation. *FEBS Letters*, *585*(24), 4018–4024. https://doi.org/10.1016/j.febslet.2011.11.014

Jagodzinski, M., Breitbart, A., Wehmeier, M., Hesse, E., Haasper, C., Krettek, C., … Hankemeier, S. (2008). Influence of perfusion and cyclic compression on proliferation and differentiation of bone marrow stromal cells in 3-dimensional culture. *Journal of Biomechanics*, *41*(9), 1885–1891. https://doi.org/10.1016/j.jbiomech.2008.04.001

Katagiri, T., Yamaguchi, A., Komaki, M., Abe, E., Takahashi, N., Ikeda, T., … Suda, T. (1994). Bone morphogenetic protein-2 converts the differentiation pathway of C2C12 myoblasts into the osteoblast lineage. *The Journal of Cell Biology*, *127*(6 Pt 1), 1755–1766. Retrieved from. http://www.pubmedcentral.nih.gov/articlerender.fcgi?artid=2120318&tool=pmcentrez&rendertype=abstract, https://doi.org/10.1083/jcb.127.6.1755

Klein, P., Schell, H., Streitparth, F., Heller, M., Kassi, J.-P., Kandziora, F., … Duda, G. N. (2003). The initial phase of fracture healing is specifically sensitive to mechanical conditions. *Journal of Orthopaedic Research: Official Publication of the Orthopaedic Research Society*, *21*(4), 662–669. https://doi.org/10.1016/S0736-0266(02)00259-0

Klein-Nulend, J., Roelofsen, J., Semeins, C. M., Bronckers, A. L., & Burger, E. H. (1997). Mechanical stimulation of osteopontin mRNA expression and synthesis in bone cell cultures. *Journal of Cellular Physiology*, *170*(2), 174–181. https://doi.org/10.1002/(SICI)1097-4652(199702)170:2<174::AID-JCP9>3.0.CO;2-L

Klosterhoff, B. S., Ghee Ong, K., Krishnan, L., Hetzendorfer, K. M., Chang, Y.-H., Allen, M. G., … Willett, N. J. (2017). Wireless implantable sensor for noninvasive, longitudinal quantification of axial strain across rodent long bone defects. *Journal of Biomechanical Engineering*, *139*(11), 111004. https://doi.org/10.1115/1.4037937

Kopf, J., Petersen, A., Duda, G. N., & Knaus, P. (2012). BMP2 and mechanical loading cooperatively regulate immediate early signalling events in the BMP pathway. *BMC Biology*, *10*(1), 37. https://doi.org/10.1186/1741-7007-10-37

Krause, C., Guzman, A., & Knaus, P. (2011). Noggin. *The International Journal of Biochemistry & Cell Biology*, *43*(4), 478–481. https://doi.org/10.1016/J.BIOCEL.2011.01.007

Lee, K. S., Kim, H. J., Li, Q. L., Chi, X. Z., Ueta, C., Komori, T., … Bae, S. C. (2000). Runx2 is a common target of transforming growth factor beta1 and bone morphogenetic protein 2, and cooperation between Runx2 and Smad5 induces osteoblast-specific gene expression in the pluripotent mesenchymal precursor cell line C2C12. *Molecular and Cellular Biology*, *20*(23), 8783–8792. Retrieved from. http://www.ncbi.nlm.nih.gov/pubmed/11073979

Li, C., Wernig, F., Hu, Y., & Xu, Q. (2003). Mechanical stress-activated PKCδ regulates smooth muscle cell migration. *Atherosclerosis Supplements*, *4*(2), 202. https://doi.org/10.1016/S1567-5688(03)90859-2

Liu, C., Abedian, R., Meister, R., Haasper, C., Hurschler, C., Krettek, C., … Jagodzinski, M. (2012). Influence of perfusion and compression on the proliferation and differentiation of bone mesenchymal stromal cells seeded on polyurethane scaffolds. *Biomaterials*, *33*(4), 1052–1064. https://doi.org/10.1016/j.biomaterials.2011.10.041

Märdian, S., Schaser, K.-D., Duda, G. N., & Heyland, M. (2015). Working length of locking plates determines interfragmentary movement in distal femur fractures under physiological loading. *Clinical Biomechanics*, *30*(4), 391–396. https://doi.org/10.1016/j.clinbiomech.2015.02.006

Mehta, M., Duda, G. N., Perka, C., & Strube, P. (2011). Influence of gender and fixation stability on bone defect healing in middle-aged rats: A pilot study. *Clinical Orthopaedics and Related Research*, *469*(11), 3102–3110. https://doi.org/10.1007/s11999-011-1914-y

Michalopoulos, E., Knight, R. L., Korossis, S., Kearney, J. N., Fisher, J., & Ingham, E. (2012). Development of methods for studying the differentiation of human mesenchymal stem cells under cyclic compressive strain. *Tissue Engineering Part C: Methods*, *18*(4), 252–262. https://doi.org/10.1089/ten.tec.2011.0347

Morlock, M., Schneider, E., Bluhm, A., Vollmer, M., Bergmann, G., Müller, V., & Honl, M. (2001). Duration and frequency of every day activities in total hip patients. *Journal of Biomechanics*, *34*(7), 873–881. Retrieved from. http://www.ncbi.nlm.nih.gov/pubmed/11410171

Nishimura, R., Hata, K., Matsubara, T., Wakabayashi, M., & Yoneda, T. (2012). Regulation of bone and cartilage development by network between BMP signalling and transcription factors. *Journal of Biochemistry*, *151*(3), 247–254. https://doi.org/10.1093/jb/mvs004

Ode, A., Kopf, J., Kurtz, A., Schmidt-Bleek, K., Schrade, P., Kolar, P., … Kasper, G. (2011). CD73 and CD29 concurrently mediate the mechanically induced decrease of migratory capacity of mesenchymal stromal cells. *European Cells and Materials*, *22*(030), 26–42. https://doi.org/10.22203/eCM.v022a03

Petersen, A., Princ, A., Korus, G., Ellinghaus, A., Leemhuis, H., Herrera, A., … Duda, G. N. (2018). A biomaterial with a channel-like pore architecture induces endochondral healing of bone defects. *Nature Communications*, *9*(1), 4430. https://doi.org/10.1038/s41467-018-06504-7

Petersen, A., Joly, P., Bergmann, C., Korus, G., & Duda, G. N. (2012). The impact of substrate stiffness and mechanical loading on fibroblast-induced scaffold remodeling. *Tissue Engineering Part a*, *18*(17–18), 1804–1817. https://doi.org/10.1089/ten.tea.2011.0514

Raeber, G. P., Lutolf, M. P., & Hubbell, J. a. (2008). Part II: Fibroblasts preferentially migrate in the direction of principal strain. *Biomechanics and Modeling in Mechanobiology*, *7*(3), 215–225. https://doi.org/10.1007/s10237-007-0090-1

Rui, Y. F., Lui, P. P. Y., Ni, M., Chan, L. S., Lee, Y. W., & Chan, K. M. (2011). Mechanical loading increased BMP-2 expression which promoted osteogenic differentiation of tendon-derived stem cells. *Journal of Orthopaedic Research: Official Publication of the Orthopaedic Research Society*, *29*(3), 390–396. https://doi.org/10.1002/jor.21218

Schell, H., Epari, D. R., Kassi, J. P., Bragulla, H., Bail, H. J., & Duda, G. N. (2005). The course of bone healing is influenced by the initial shear

fixation stability. *Journal of Orthopaedic Research*, *23*(5), 1022–1028. https://doi.org/10.1016/j.orthres.2005.03.005

Schell, H., Thompson, M. S., Bail, H. J., Hoffmann, J. E., Schill, A., Duda, G. N., & Lienau, J. (2008). Mechanical induction of critically delayed bone healing in sheep: Radiological and biomechanical results. *Journal of Biomechanics*, *41*(14), 3066–3072. https://doi.org/10.1016/j.jbiomech.2008.06.038

Shi, Y., Li, H., Zhang, X., Fu, Y., Huang, Y., Lui, P. P. Y., … Dai, K. (2011). Continuous cyclic mechanical tension inhibited Runx2 expression in mesenchymal stem cells through RhoA-ERK1/2 pathway. *Journal of Cellular Physiology*, *226*(8), 2159–2169. https://doi.org/10.1002/jcp.22551

Shin Kang, K., Hun Jeong, Y., Min Hong, J., Yong, W.-J., Rhie, J.-W., & Cho, D.-W. (2013). Flexure-based device for cyclic strain-mediated osteogenic differentiation. *Journal of Biomechanical Engineering*, *135*(11), 114501. https://doi.org/10.1115/1.4025103

Sittichokechaiwut, A., Edwards, J. H., & Scutt, a M., & Reilly, G. C. (2010). Short bouts of mechanical loading are as effective as dexamethasone at inducing matrix production by human bone marrow mesenchymal stem cell. *European Cells & Materials*, *20*, 45–57. https://doi.org/10.22203/eCM.v020a05

Sliogeryte, K., Thorpe, S. D., Lee, D. A., Botto, L., & Knight, M. M. (2014). Stem cell differentiation increases membrane-actin adhesion regulating cell blebability, migration and mechanics. *Scientific Reports*, *4*, 7307. https://doi.org/10.1038/srep07307

Sumanasinghe, R. D., Bernacki, S. H., & Loboa, E. G. (2006). Osteogenic differentiation of human mesenchymal stem cells in collagen matrices: effect of uniaxial cyclic tensile strain on bone morphogenetic protein (BMP-2) mRNA expression. *Tissue Engineering*, *12*(12), 3459–3465. https://doi.org/10.1089/ten.2006.12.3459

Toma, C. D., Ashkar, S., Gray, M. L., Schaffer, J. L., & Gerstenfeld, L. C. (1997). Signal transduction of mechanical stimuli is dependent on microfilament integrity: Identification of osteopontin as a mechanically induced gene in osteoblasts. *Journal of Bone and Mineral Research: The Official Journal of the American Society for Bone and Mineral Research*, *12*(10), 1626–1636. https://doi.org/10.1359/jbmr.1997.12.10.1626

Tsuji, K., Bandyopadhyay, A., Harfe, B. D., Cox, K., Kakar, S., Gerstenfeld, L., … Rosen, V. (2006). BMP2 activity, although dispensable for bone formation, is required for the initiation of fracture healing. *Nature Genetics*, *38*(12), 1424–1429. https://doi.org/10.1038/ng1916

Turner, C., Owan, I., Alvey, T., Hulman, J., & Hock, J. (1998). Recruitment and proliferative responses of osteoblasts after mechanical loading in vivo determined using sustained-release bromodeoxyuridine. *Bone*, *22*(5), 463–469. https://doi.org/10.1016/S8756-3282(98)00041-6

Wang, L., Zhang, X., Guo, Y., Chen, X., Li, R., Liu, L., … Zhang, Y. (2010). Involvement of BMPs/Smad Signaling Pathway in Mechanical Response in Osteoblasts. *Cellular Physiology and Biochemistry*, *26*(106), 1093–1102. https://doi.org/10.1159/000323987

Witt, F., Duda, G. N., Bergmann, C., & Petersen, A. (2014). Cyclic mechanical loading enables solute transport and oxygen supply in bone healing: An *in vitro* investigation. *Tissue Engineering Part a*, *20*, 3–4. 140120073517006. https://doi.org/10.1089/ten.tea.2012.0678

Wulsten, D., Glatt, V., Ellinghaus, A., Schmidt-Bleek, K., Petersen, A., Schell, H., … Duda, G. N. (2011). Time kinetics of bone defect healing in response to BMP-2 and GDF-5 characterised by in vivo biomechanics. *European Cells & Materials*, *21*, 177–192. Retrieved from. http://www.ncbi.nlm.nih.gov/pubmed/21312163

Yang, K., Tang, X.-D., Guo, W., Xu, X.-L., Ren, T.-T., Ren, C.-M., … Sun, K.-K. (2016). BMPR2-pSMAD1/5 signaling pathway regulates RUNX2 expression and impacts the progression of dedifferentiated chondrosarcoma. *American Journal of Cancer Research*, *6*(6), 1302–1316. Retrieved from. http://www.pubmedcentral.nih.gov/articlerender.fcgi?artid=4937734&tool=pmcentrez&rendertype=abstract

SUPPORTING INFORMATION

Additional supporting information may be found online in the Supporting Information section at the end of the article.

Figure S1: Schematic drawing of the 3D migration assay showing all steps from cell seeding to image acquisition via fluorescence microscopy. Cell suspension was seeded inside silicone rings and cells were allowed to adhere for 1 hr. Silicone rings were removed, unattached cells were washed off, and pre-wetted scaffolds were placed on the multicell layer before culture medium was added and scaffolds were incubated for 24 hr. Scaffolds with cells attached to the bottom side were transferred into the bioreactor (with/without cyclic compression) or in well plates for static culture and incubated for 3 days. Cells were fixated, scaffolds were cut, and cyrosections (20 μm) were prepared at the mid-plane of the scaffold. Cell nuclei were stained with DAPI and overview images were recorded via a fluorescence microscope to calculate the median migration distance from the relative distance of the nuclei to the base of the scaffold (Y_0). The scaffold border areas were excluded from the measurement to avoid boundary effects. Only the ROI, indicated by the red dotted line, was analyzed.

Figure S2: Experimental setup of the oxygen concentration measurement inside cell seeded collagen scaffolds. The oxygen probe (arrow) was inserted into the upper plunger piston of the bioreactor, and the penetration depth of the probe into the scaffold was adjusted computer controlled using the bioreactors piezo drive.

Figure S3: ALP activity [nmol/min] measurement after a culture time of 7 days in osteogenic medium. The ALP activity relative to the cell metabolism measured by AlamarBlue® was determined and the fold change in relation to the untreated control (cultured in expansion medium) was calculated. Box and whisker plots depict the following values from bottom to top: minimum value, low quartile, median, upper quartile, and maximum value. Statistical significance was tested via Mann–Whitney test (two-sided) with Bonferroni correction, $^{***}p \leq 0.001$.

Figure S4: Gene expression changes of TGFβ1, TGFβ3, FGF2, PDGF-A, and VEGF-A, growth factors that influence osteogenic differentiation. Under R_{high} conditions, only TGFβ3 expression is slightly increased in response to cyclic compression. Human BMSCs were seeded in collagen scaffolds (12.4 kPa) and stimulated with and without cyclic compression (f = 1 Hz, ε = 10%) under increased cell-to-medium ratio or under concurrent rhBMP2 (5 nM) stimulation. Fold change gene expression was analyzed by qPCR in comparison with the untreated control (low cell-to-medium ratio, without cyclic compression). HPRT1 was used as the reference gene (n = 5 hBMSC donors). Statistical significance was tested via Mann–Whitney test (two-sided) with Bonferroni correction.

Figure S5: BMP2 stability during bioreactor culture. Bioreactor experiment without cultivation of cells. Recombinant hBMP2 (135 ng/ml) was added at Day 0 and medium samples were taken after 30 min (0d), on Days 1, 3, 5, and 7 to measure the BMP2 concentration [pg/ml] by ELISA. Expansion medium without additional supplements served as a control (n = 2).

How to cite this article: Schreivogel S, Kuchibhotla V, Knaus P, Duda GN, Petersen A. Load-induced osteogenic differentiation of mesenchymal stromal cells is caused by mechano-regulated autocrine signaling. *J Tissue Eng Regen Med*. 2019;13: 1992–2008. https://doi.org/10.1002/term.2948